Sea-level rise and the emergence of a keystone grazer alter the geomorphic evolution and ecology of southeast US salt marshes

Sinéad M. Crotty[a,b,1], Collin Ortals[c], Thomas M. Pettengill[d], Luming Shi[c], Maitane Olabarrieta[c], Matthew A. Joyce[e], Andrew H. Altieri[a], Elise Morrison[f], Thomas S. Bianchi[f], Christopher Craft[g], Mark D. Bertness[d], and Christine Angelini[a,c]

[a]Department of Environmental Engineering Sciences, Engineering School of Sustainable Infrastructure and Environment, University of Florida, Gainesville, FL 32611; [b]School of the Environment, Yale University, New Haven, CT 06511; [c]Department of Coastal Engineering, Engineering School of Sustainable Infrastructure and Environment, University of Florida, Gainesville, FL 32611; [d]Department of Ecology and Evolutionary Biology, Brown University, Providence, RI 02912; [e]Department of Biosciences, Swansea University, Singleton Park, Swansea SA28PP, United Kingdom; [f]Department of Geological Sciences, University of Florida, Gainesville, FL 32611; and [g]School of Public and Environmental Affairs, Indiana University Bloomington, Bloomington, IN 47405

Edited by Mary E. Power, University of California, Berkeley, CA, and approved June 9, 2020 (received for review October 15, 2019)

Keystone species have large ecological effects relative to their abundance and have been identified in many ecosystems. However, global change is pervasively altering environmental conditions, potentially elevating new species to keystone roles. Here, we reveal that a historically innocuous grazer—the marsh crab *Sesarma reticulatum*—is rapidly reshaping the geomorphic evolution and ecological organization of southeastern US salt marshes now burdened by rising sea levels. Our analyses indicate that sea-level rise in recent decades has widely outpaced marsh vertical accretion, increasing tidal submergence of marsh surfaces, particularly where creeks exhibit morphologies that are unable to efficiently drain adjacent marsh platforms. In these increasingly submerged areas, cordgrass decreases belowground root:rhizome ratios, causing substrate hardness to decrease to within the optimal range for *Sesarma* burrowing. Together, these bio-physical changes provoke *Sesarma* to aggregate in high-density grazing and burrowing fronts at the heads of tidal creeks (hereafter, creekheads). Aerial-image analyses reveal that resulting "*Sesarma*-grazed" creekheads increased in prevalence from 10 ± 2% to 29 ± 5% over the past <25 y and, by tripling creek-incision rates relative to nongrazed creekheads, have increased marsh-landscape drainage density by 8 to 35% across the region. Field experiments further demonstrate that *Sesarma*-grazed creekheads, through their removal of vegetation that otherwise obstructs predator access, enhance the vulnerability of macrobenthic invertebrates to predation and strongly reduce secondary production across adjacent marsh platforms. Thus, sea-level rise is creating conditions within which *Sesarma* functions as a keystone species that is driving dynamic, landscape-scale changes in salt-marsh geomorphic evolution, spatial organization, and species interactions.

biodiversity | bioturbation | ecosystem engineer | herbivory | morphodynamics

Climate change and other human disturbances are widely redefining species distributions and environmental conditions, thereby modifying the organization of our world's oceans, forests, grasslands, wetlands, tundras, and reefs (1–4). A potentially critical consequence of these changes is a shift in the importance and identity of keystone species—those species whose ecological effects are large relative to their abundance and/or biomass (5, 6) and whose functional roles, like all other species, are context-dependent and, hence, sensitive to physical and biotic conditions (5, 7–9). In many systems, predators that once filled keystone roles, such as sea otters (10), wolves (11), and large-mouth bass (12), are functionally extinct in much of their historic range, causing profound changes in biodiversity and ecosystem processes (10, 11, 13). Simultaneously, the ecological effects of other species and functional groups potentially less vulnerable to exploitation or habitat loss, such as mutualists and grazers, are strengthening with global change, even in locations with robust predator populations (14–16). Together, these shifting dynamics are challenging scientists to evaluate whether the rules previously shown to control community pattern generation still apply, and to revise their perceptions and designations of keystone species even in the most well-studied ecosystems (2, 3, 17, 18).

Coastal habitats are among the most productive, economically valuable, and intensively researched ecosystems on Earth (19–21). They are also relevant systems for detecting whether global change factors are activating emergent keystone species that, in turn, alter ecological dynamics and geomorphic processes. This is because novel physical and biotic conditions are governing these ecosystems in the Anthropocene. Many coastal predator populations are depressed (13, 17), and eutrophication, drought, increased storm frequency and intensity, and sea-level rise pervasively influence estuarine and nearshore hydrodynamics,

Significance

Human disturbances, climate change, and their combined effects on species distributions and environmental conditions are increasingly modifying the organization of our world's oceans, forests, grasslands, wetlands, tundras, and reefs. Here, we reveal that these contemporary conditions can trigger the emergence of novel keystone species. Across the southeastern US coastal plain, sea-level rise is outpacing salt marsh vertical accretion, causing these grasslands to be tidally inundated for longer and softening marsh substrates to levels optimal for crab burrowing. Using field experiments, measurements, surveys, and models, we show that these conditions amplify the burrowing and grazing effects of a previously inconspicuous crab, enabling it to redefine predator–prey interactions, eco-geomorphic feedbacks, and the mechanisms by which salt marshes are responding to climate change.

Author contributions: S.M.C., T.M.P., and C.A. designed research; S.M.C., T.M.P., M.A.J., and C.C. performed research; S.M.C., C.O., L.S., and M.O. analyzed data; and S.M.C., A.H.A., E.M., T.S.B., M.D.B., and C.A. wrote the paper.

The authors declare no competing interest.

This article is a PNAS Direct Submission.

Data deposition: All datasets are freely available at https://doi.org/10.6084/m9.figshare.12581579.v1.

[1]To whom correspondence may be addressed. Email: sinead.crotty@yale.edu.

This article contains supporting information online at https://www.pnas.org/lookup/suppl/doi:10.1073/pnas.1917869117/-/DCSupplemental.

sediment transport processes, and species composition from the bottom up (17, 22–24). Where these conditions decrease survivorship of the ecosystem-defining foundation species (e.g., oysters, corals, mangroves, seagrasses, and dune-building grasses), biodiversity loss and changes to eco-geomorphic feedbacks are often observed (25–27).

Among the most visually striking and morphodynamically impactful disturbances in US Atlantic salt marshes are those generated by the purple marsh crab, *Sesarma reticulatum* (hereafter *Sesarma*). This grazer consumes foundational cordgrass (*Spartina alterniflora*) both aboveground and belowground (i.e., leaves, roots, and rhizomes) and excavates burrows as deep as 0.5 m (28–33). Since the 1970s, high-density *Sesarma* fronts that leave denuded, burrow-riddled creekbanks in their wake (34) have been documented from New York to Massachusetts (35), particularly where recreational fishing has extirpated *Sesarma*'s predators (36). In the northeastern United States, *Sesarma* fronts form exclusively on lower-elevation creekbanks, where elevated water velocities flush sediment and toxins from their burrows, *Sesarma* recruitment rates are high, and marsh substrates exhibit suitable hardness (~1.4 $kg{\cdot}cm^{-2}$) for *Sesarma* burrow excavation and maintenance (37). On adjacent, higher-elevation marsh platforms, dense root mats cause the substrate to be too hard for *Sesarma* burrowing (>2 $kg{\cdot}cm^{-2}$; refs. 29 and 37). Recent research has suggested that if sea-level rise outpaces salt-marsh vertical accretion, the resulting extension in the duration of tidal flooding will drive a shift in plant-tissue allocation from dense-packed fine roots to larger rhizomes that better aerate the soil and increase pore space, thereby softening the marsh platform and enhancing the system's overall vulnerability to *Sesarma* intensive burrowing and overgrazing (29). However, these forecasts have yet to be confirmed or explored in other regions.

At lower latitudes in the >1 million acres of South Carolina, Georgia, and northern Florida salt marshes, predator populations (e.g., red drum, blue crabs, and diamondback terrapins) are generally depressed relative to preindustrial levels (38, 39), but still exert strong top-down control of *Sesarma* (*SI Appendix*, Fig. S1) and other macrobenthic invertebrates (22). Despite robust predation pressure, *Sesarma* fronts have been noted at few isolated sites in the southeastern United States, but are limited to headward margins of creeks where tidewater floods onto and drains off of salt marsh platforms (hereafter, "creekheads") (31–33). On creekheads where water velocities are particularly high, *Sesarma* grazing and burrowing increase water infiltration, organic matter decomposition, and sediment export, causing the marsh platform to erode into incising creeks (32, 33). Similar to creek-formation dynamics moderated by herbivorous burrowing crabs in Argentinean salt marshes (40, 41), sea-level rise outpacing salt marsh vertical accretion is hypothesized to fuel *Sesarma* front propagation and creek growth in the southeastern United States by burdening creeks with larger volumes of water to exchange (31–33).

However, no studies have explored whether *Sesarma* impacts on salt marsh geomorphology are regionally prevalent; whether they are escalating in concert with sea-level rise; or how they may influence community structure, species interactions, and ecosystem functions on scales that extend beyond their limited spatial footprint (grazed creekheads only cover ~1% of total marsh area). To address these knowledge gaps and evaluate how global change may be redefining the ecological role of *Sesarma* from being a burrowing grazer with modest community- and ecosystem-level impacts (42–49) to a keystone species at the creekshed scale, we conducted aerial-image analyses, Regional Ocean Modeling System (ROMS) simulations, surveys, mortality assays, and field experiments. We conclude that sea-level rise is triggering the emergence of *Sesarma* as a regionally impactful keystone species that is controlling salt marsh geomorphic evolution and ecological structure at scales disproportionate to its abundance and spatial coverage in the system.

Results and Discussion

Sea-Level Rise, Marsh Accretion, and Tidal Submergence. To explore how sea-level rise may be altering physical and biotic conditions that govern *Sesarma*'s functionality and the structure of southeastern US salt marshes, we first evaluated historic changes in sea levels and marsh vertical-accretion rates from South Carolina to northern Florida—a region defined by similar geological, riverine, and tidal forcing (50). To do so, we obtained hourly historic sea-level data from the three National Oceanographic and Atmospheric Administration (NOAA) tide stations in the region: Charleston, Cooper River Entrance, SC; Fort Pulaski, GA; and Fernandina Beach, FL. For the same region, we collected all available measurements of salt marsh platform vertical-accretion rates collected via radiometric dating of soil cores (^{210}Pb and ^{137}Cs), which estimate accretion on multidecadal timescales, as well as feldspar marker horizon (51) and sediment elevation table (SET) measurements, which provide shorter-term (annual to decadal timescale) measures of accretion.

Between 1940 and 1998, the period preceding that which covers our aerial-image analyses (detailed below) and a time over which no records of *Sesarma*-grazed creekheads occur in the literature (refs. 42–49 and *SI Appendix*, *Methods*), sea level rose at an average rate of 2.6 ± 0.2 $mm{\cdot}y^{-1}$ (mean ± SE, here and below) across the region (Fig. 1*A*), ranging from 2.1 $mm{\cdot}y^{-1}$ in Fernandina Beach (FL) to 2.9 $mm{\cdot}y^{-1}$ in Fort Pulaski (GA). Over the last two decades (1999 to 2019), sea level increased at rates 2.2 to 2.6 times faster than the preceding period, averaging 6.1 ± 0.7 $mm{\cdot}y^{-1}$ across the region (Fig. 1*A*). Across all measurements, salt-marsh vertical accretion rate averaged 2.1 ± 0.3 $mm{\cdot}y^{-1}$ and varied considerably among sampled sites (Fig. 1*B* and *SI Appendix*, *Methods* and Table S1). Of the 55 collated vertical accretion measurements, 35% (19 of 55) exceeded the rate of relative sea-level rise recorded at the nearest NOAA tide station during the 1940 to 1998 time period, while only 3.6% (2 of 55) exceeded relative sea-level rise in the 1999 to 2019 time period (Fig. 1*B*). These results suggest that while sea-level rise and salt marsh vertical accretion were historically in near-equilibrium at some sites in the region, this has not been the case over the last two decades. Instead, most salt-marsh platforms appear to be gradually drowning due to sea-level rise outpacing marsh vertical accretion in recent decades.

To explore how these trends in sea level and vertical marsh accretion may be altering the duration that salt marshes are tidally submerged, we developed first-order approximation estimates of average daily submergence time (hours per day) at marsh creekhead elevations. Using five representative vertical-accretion scenarios and the sea-level data recorded at the Fort Pulaski (GA) tide station, we estimated tidal submergence for each year during the 1940 to 1998 and the 1999 to 2019 time periods. In the 0- to 2.5-$mm{\cdot}y^{-1}$ accretion scenarios representative of two-thirds of vertical-accretion rates in our regional database (Fig. 1*B* and *SI Appendix*, Table S1), we estimated that the marsh surface was tidally submerged for 0.4 to 1.8 more hours per day in 1998 compared to 1940 (Fig. 1*C*). In accretion scenarios of 2.9 and 4.0 $mm{\cdot}y^{-1}$, representative of the minority of marshes accreting at rates equivalent to or faster than mean sea-level rise, we estimated that the marsh surface was tidally submerged for 0.6 fewer hours or the same number of hours per day, respectively, in 1998 compared to 1940 (Fig. 1*C*). During the 1999 to 2019 period, however, salt marshes in all five vertical-accretion scenarios experienced an increase in submergence, with daily inundation time increasing 2- to 55-fold relative to the 1940 to 1998 time period. In these simulations, the marsh was tidally submerged for 0.6 to 1.1 more hours per day (minimum- and maximum-accretion scenarios, respectively),

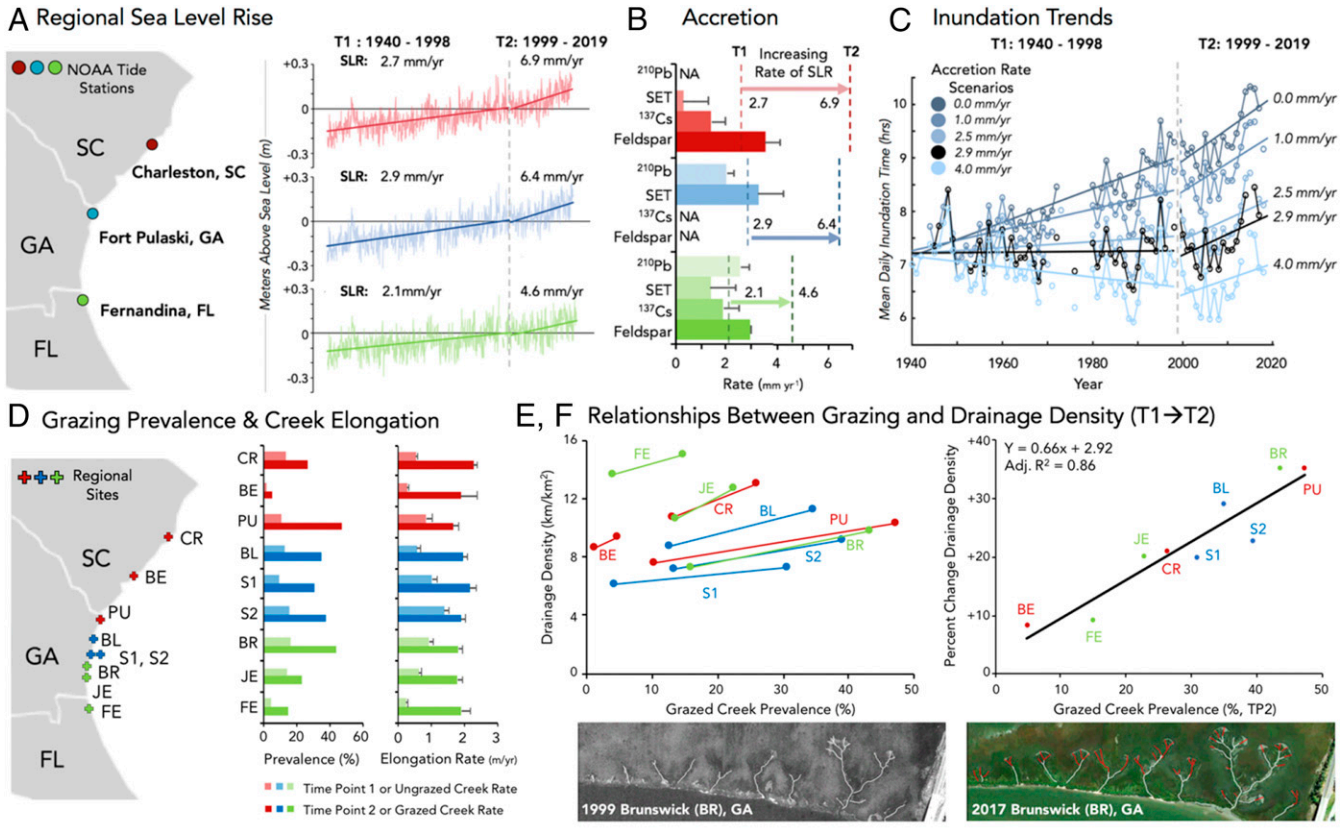

Fig. 1. Sea-level rise, submergence, and *Sesarma*-grazing trends. (*A*) Relative sea-level rise recorded at the Charleston, SC (northern; red); Fort Pulaski, GA (central; blue); and Fernandina Beach, FL (southern; green) NOAA tide stations from 1940 to 2019. Trend lines and black text denote the average annual rate of sea-level rise (SLR) during the 1940 to 1998 (T1) and 1999 to 2019 (T2) time periods. (*B*) Rates of salt-marsh-platform vertical accretion measured via ^{210}Pb, SET, ^{137}Cs, and Feldspar marker horizon methods are shown as mean + SE for each method for salt marshes located in each subregion. Dashed lines refer to the relative rate of sea-level rise in each subregion at T1 and T2. (*C*) First-order approximations of the duration of tidal submergence, or inundation time (hours per day), experienced by salt-marsh creekheads under each of five marsh vertical accretion-rate scenarios. The dashed gray line denotes the boundary of T1 and T2. (*D*) Aerial-image analysis of 1-km^2 areas at each of nine sites (site name abbrevations are reported inset and across panels) revealed that grazed creek prevalence increased at all sites between TP1 (light shading) and TP2 (dark shading) and that the elongation rate between the two time points is faster for grazed creeks than ungrazed creeks in all locations. (*E*) At all sites, marsh-drainage density increased with the rise in grazed creek prevalence observed between TP1 and TP2. (*F*) Across all sites, grazed creek prevalence at TP2 strongly predicted the percent change in drainage density between the two time points. Model results are presented (inset) and aerial images depicting changes in creek length between TP1 and TP2 are shown (*E* and *F*, *Lower*).

leading to an increase of 219 to 402 h of tidal submergence annually, in 2019 as compared to 1999.

Grazing Prevalence, Creek Elongation, and Marsh Drainage Density. Next, to quantify the potential impacts of sea-level rise outpacing marsh accretion on the prevalence of *Sesarma*-grazed creekheads, we examined whether *Sesarma*-grazed creekheads became more common features over the last two decades. By counting and ground-truthing the number of grazed and ungrazed creekheads in 1-km^2 replicate areas delineated in aerial images at nine sites distributed along the South Carolina–Florida coastline (Fig. 1*D* and *SI Appendix*, Table S2), we discovered that the proportion of creekheads grazed by *Sesarma* increased at all sites and by an average of 240 ± 52% between time point 1 (TP1; 1994 or 1999, depending on image availability) and time point 2 (TP2; 2016, 2017, or 2018; time point: $F_{1,16} = 15.6$; $P = 0.001$). In TP1, only 1 to 16% of creekheads were grazed, but by TP2, between 5% and 47% of creekheads were grazed at each site (Fig. 1*D*). By measuring the length of every creek at each time point, we further discovered that grazed creeks incised into marsh platforms more than three times faster (1.91 ± 0.06 m·y^{-1}; mean ± SE) than ungrazed creeks (0.61 ± 0.03 m·y^{-1}) at all nine sites (Creek Status at TP2: $F_{1,905} = 248.0$; $P < 0.0001$; Tukey's honest significant difference [HSD], $P < 0.01$).

To evaluate how *Sesarma*-mediated changes in creek incision rates collectively influence salt marsh geomorphic structure at landscape scales, we calculated the creek-drainage density of the nine 1-km^2 regional sites—i.e., the total length of tidal creeks divided by the marsh area the creeks drain—at each time point (Fig. 1*E*). We found that the creek drainage density increased by 8 to 35% across all sites between TP1 and TP2, with total tidal creek length increasing annually at a rate of 102 ± 12 m·km^{-2} marsh platform per year, and by 1.9 ± 0.2 km·km^{-2} marsh platform over the entire <25-y period. Moreover, the percent change in drainage density between TP1 and TP2 increased positively and linearly with grazing intensity (percent creeks grazed) at TP2 (Fig. 1*F*; $P < 0.001$; adjusted $R^2 = 0.86$), such that sites with highest proportions of *Sesarma*-grazed creekheads experienced the largest increases in drainage density. These results reveal that, over the past two decades, *Sesarma*-grazed creekheads consistently increased in prevalence and, despite occupying <1% of total marsh area, have rapidly altered the geospatial evolution of salt marshes across the region by accelerating creek growth and enhancing marsh drainage density.

Geospatial Drivers of *Sesarma*-Grazed Creekhead Distribution. Next, to assess whether the spatial distribution of *Sesarma*-grazed creekheads are nonrandom and predictably related to marsh geomorphic features known to control tidewater flooding and draining dynamics—and may thus be modulating the effect of sea-level rise on marsh submergence—we measured both the length and associated creekshed area of a subset of creeks measured in the aerial-image analyses. We focused on creek length because it is an easy-to-measure feature that positively correlates with creek cross-sectional area and the volume of water exchanged per unit time by a creek (52–56). We then estimated the creekshed area of each creek based on proximity to upland borders and other drainage features, and we used this variable as a measure of the tidewater burden experienced by each creek (53). For each creek and time point, we divided the creekshed area by creek length to calculate the "drainage ratio," a measure of the marsh area drained per meter of creek. We hypothesized that *Sesarma*-grazed creekheads would occur on creeks exhibiting high drainage ratios—i.e., in areas where the creek's hydraulic capacity is too small to efficiently drain tidewater from the adjacent marsh. In support of this hypothesis, we discovered that the drainage ratios of grazed creeks (848.7 m^2 creekshed per m of tidal creek) and incipient-grazed creeks (930.0 m^2 creekshed per m of tidal creek) were more than six times higher than those of ungrazed creeks (132.0 m^2 creekshed per m of tidal creek) of similar lengths (Tukey's HSD, $P < 0.01$; Fig. 2*A*; $n = 60$ creeks).

Further, to evaluate whether there exists a threshold drainage ratio above which *Sesarma* fronts are established, we first identified the marginal creeks—the five ungrazed creeks with the highest drainage ratios and the five incipient-grazed creeks with the lowest drainage ratios. We then used linear regression analyses between creek length and creekshed area for each set of marginal creeks. The slope (i.e., creekshed area/creek length), or the "drainage ratio," of the marginal ungrazed creeks regression line was 265.9 m^2 per m of tidal creek, while the slope (i.e., "drainage ratio") of the marginal incipient-grazed creeks was 266.8 m^2 per m of tidal creek (Fig. 2*B*). Thus, these analyses suggest a threshold drainage ratio of ~266 m^2 per m of creek, above which *Sesarma* grazing is likely to occur.

Given that creeks with grazed creekheads rapidly incise into adjacent marshes (Fig. 1*D*), their lengths invariably increase with time. As a result, drainage ratios of grazed creeks generally decrease over time. To explore if *Sesarma* fronts fail to persist on creeks whose drainage ratio has shifted from being above to below the aforementioned threshold (as a result of creek elongation), we selected five creeks that were rapidly elongating and grazed by *Sesarma* in 1999, but whose elongation rate had slowed and where grazing declined to such a degree that cordgrass revegetated the former grazing front by 2019. We measured the drainage ratios of these creeks at both time points. In all five cases, the creeks exhibited drainage ratios higher than the threshold in 1999 (452 ± 87 m^2 per m of tidal creek) and less than the threshold in 2019 (201 ± 22 m^2 per m of tidal creek; Fig. 2*C*). We draw two conclusions from these results. First, simple relationships between the hydraulic capacity of creeks and the area of marsh that they drain appear to explain where *Sesarma* aggregate in high enough densities on creekheads to initiate eco-geomorphic feedbacks that accelerate creek incision in salt marshes across the region. Second, once grazed creeks achieve sufficient hydraulic capacity to adequately drain adjacent marsh areas, tidal-submergence levels and tidal-flow velocities appear to become unsuitable for sustaining *Sesarma* front formation, causing creek elongation to slow and cordgrass to revegetate the previously denuded creekhead.

Creek Morphology, Tidal Submergence, and Marsh Softening. To quantify the potential effects of drainage ratio on tidal submergence times, we applied the ROMS (57, 58). Models consisted of a main channel, marsh platform, tidal creek, and outer

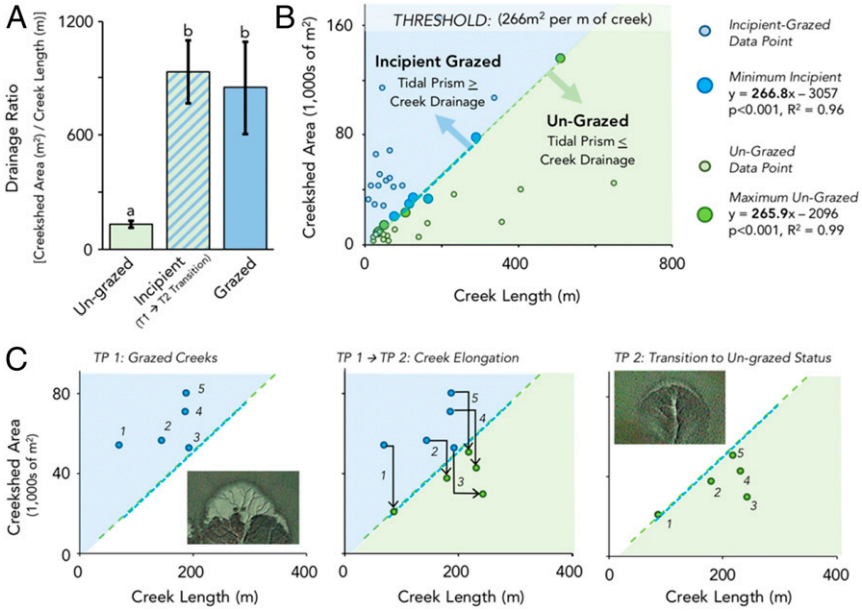

Fig. 2. Geospatial drivers of *Sesarma*-grazed creekhead distribution. (*A*) Drainage ratios of grazed and incipient-grazed creeks were six times higher than those of ungrazed creeks. (*B*) Marginal incipient-grazed creeks (five minimum drainage ratios) and ungrazed creeks (five maximum drainage ratios) were assessed by using linear regression analyses. Results identified a threshold drainage ratio of 266 m^2 per m tidal creek (dashed blue and green regression lines). Above this line, we suggest that the volume of water that requires drainage per tidal cycle (i.e., tidal prism) is greater than the creek-drainage capacity, and, as a result, grazing is likely to initiate. Below this line, the creek's hydraulic capacity is sufficient to drain the adjacent marsh platform, and the creek remains ungrazed. (*C*) Five creeks with a history of grazing at TP1 that transitioned to an ungrazed status at TP2 show that this transition away from grazing coincides with the creek transitioning from above to below the identified threshold drainage ratio.

marsh levees. To evaluate the effects of changing the drainage ratio, three idealized model bathymetries were considered. The bathymetries shared the same channel, levees, and marsh-platform areas, but differed in the length of the tidal creek, such that their drainage ratios were 849; 266; and 132 m^2 per m of tidal creek—the drainage ratios of grazed, threshold, and ungrazed conditions, respectively (Fig. 3 *A*–*C*). To assess differences in tidal submergence of marsh platforms, we selected a point on the marsh surface, standardized for elevation (+0.70 m above sea level [ASL]) and distance from creekhead (20 m) in each scenario, and quantified the total number of hours that point was submerged during one tidal cycle (Fig. 3*D*). Grazed (7.45 h) and threshold (5.33 h) marsh platforms were inundated for 110% and 50% longer than ungrazed creeks (3.78 h), respectively. To then estimate how relative sea-level rise has altered marsh submergence times, we simulated tidal exchange over the threshold marsh scenario at three timepoints: 1940, 1999, and 2019 (Fig. 3 *E*–*G*). We found that our focal point on the marsh platform was inundated for 4% more time in 1999 than in 1940 and for 17% more time on average in 2019 compared to 1940 (Fig. 3*H*). When scaled annually, this focal point on threshold marsh platforms was inundated for >141 more hours in 1999 and >550 more hours per year in 2019 as compared to 1940, further highlighting that the recent acceleration in sea-level rise (Fig. 1) is likely significantly extending the duration that salt marshes in the region are tidally submerged.

To ground-truth these geomorphology-based predictions, we conducted field surveys of elevation, submergence time, tidewater flow rates, and substrate hardness on grazed, ungrazed, and incipient-grazed creekheads and adjacent marsh platforms (*SI Appendix*, *Methods*). As predicted, surveys revealed that grazed creekheads are submerged for longer, experience faster tidewater flows, and exhibit softer substrates at standardized elevations and distances from creekheads than their ungrazed counterparts (*SI Appendix*, Fig. S2). Soil cores taken from grazed and ungrazed creekhead borders and marsh platforms further suggest that the softening of marsh-platform substrates in part results from a decrease in cordgrass root to rhizome ratio when located in close proximity to a grazing front (multiple regression: $F_{3,59} = 37.55$; $P < 0.0001$; *SI Appendix*, Fig. S3).

Taken together, our estimates of changes in tidal submergence, aerial-image analyses, drainage-ratio calculations, ROMS simulations, and field measurements indicate that: 1) sea-level rise is enhancing the tidewater burden experienced by salt marshes across the region; 2) this burden is heterogeneously (but predictably) distributed across marsh platforms and is promoting the establishment of *Sesarma* fronts on creeks with high drainage ratios, longer submergence times, faster water velocities, and softened substrates; and 3) once formed, *Sesarma* fronts are modifying the response of salt marshes to rising sea levels by lengthening individual creeks, enhancing their hydraulic-exchange capacity, and increasing the drainage efficiency of these intertidal landscapes as a whole. Although it is possible that *Sesarma* fronts are forming due to other environmental factors, all of these results, as well as our finding that this crab species fails to sustain coherent fronts where the drainage ratios fall below our calculated threshold drainage ratio value, suggest that sea-level rise is the principle driver of the eco-morphic feedbacks we document in this study.

***Sesarma* Effects on Community Structure and Species Interactions.** Where grazing fronts are established, *Sesarma* actively remove the 1- to 2-m-tall cordgrass along creekheads, vegetation that functions as a barrier to nekton predator access into the marsh

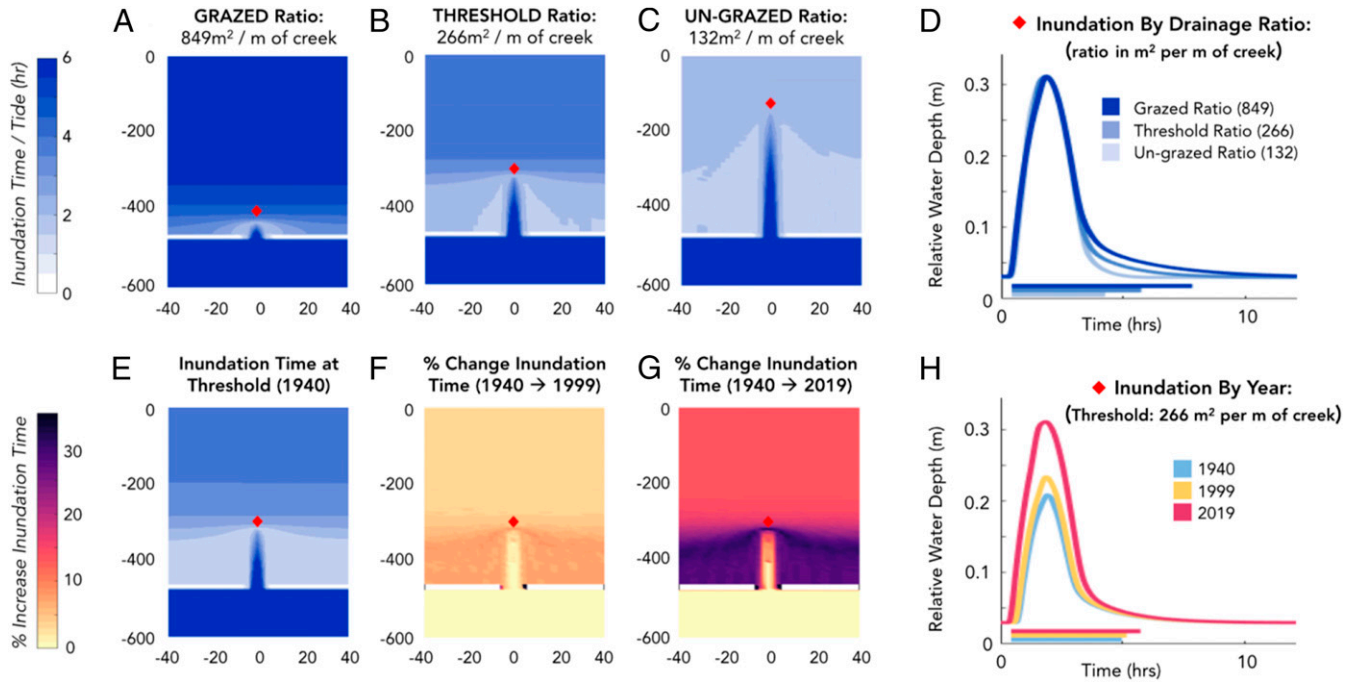

Fig. 3. ROMS simulations. (*A*–*C*) ROMS simulations were conducted by using three idealized model bathymetries that differed only in the length of the tidal creek, such that their drainage ratios were those of grazed (*A*; 849 m^2 per m of tidal creek), threshold (*B*; 266 m^2 per m of tidal creek), and ungrazed conditions (*C*; 132 m^2 per m of tidal creek). Submergence, or inundation time, is presented on a scale of blue color, with darker hues representing longer periods of submergence. In all panels, a location standardized for elevation (+0.70 m ASL) and proximity to tidal creekhead (20 m) is shown as a red diamond. (*D*) Inundation time at this reference point is presented for the three bathymetries. (*E*) Adjusting the elevation of the threshold simulation for relative rates of sea-level rise, inundation time is presented for the threshold drainage ratio in 1940. (*F* and *G*) Percent increases in inundation time between 1940 and both 1999 (*F*) and 2019 (*G*) are depicted on a color scale of yellow (low) to red (intermediate) to purple (high). (*H*) Changes in inundation time at the reference point are shown between 1940, 1999, and 2019.

(59). As a result, we hypothesized that *Sesarma*-grazed creekheads may alter the spatial distribution of resident marsh fauna that function as a prey base for many commercially and recreationally harvested coastal predators and mediate ecosystem functions (43, 60). To test this prediction, we surveyed dominant macrobenthic invertebrate community composition and biomass in marsh platform areas adjacent to tidal creeks. Benthic invertebrate community biomass levels did not vary by site (site: $P > 0.09$), but within sites were >600% higher on ungrazed marsh borders (i.e., locations immediately adjacent to creekheads) and 300% higher on ungrazed marsh platforms than grazed marsh borders and grazed marsh platforms, respectively (Marsh type*Zone: $F_{1,284} = 60.5$, $P < 0.0001$, Tukey's HSD $P < 0.01$; Fig. 4 *A*–*C* and *SI Appendix*, Fig. S4). Elevated ribbed mussel (*Geukensia demissa*) abundance on ungrazed marsh borders and, to a lesser degree, on ungrazed marsh platforms drove much of these differences in benthic invertebrate community biomass, although higher abundances of all functional groups, except *Sesarma*, occurred on ungrazed compared to grazed marsh borders and platforms (Fig. 4*C* and *SI Appendix*, Fig. S4). *Sesarma*, in contrast, was 80 times more abundant on grazed borders than the other surveyed marsh locations (Tukey's HSD, $P < 0.01$; Fig. 4*C* and *SI Appendix*, Fig. S4).

Since removal of the cordgrass canopy by *Sesarma* grazing at the creekhead likely increases predator access to invertebrate prey, we assessed whether the substantially reduced mussel biomass observed in grazed marshes (Fig. 4*C*) could be explained by variation in predation pressure. We deployed mussels in aggregations to mimic their natural, clustered distribution (60, 61) in the border and platform zones of grazed and ungrazed marshes, paired within three Sapelo Island, GA, sites ($n = 8$ mussel aggregations each per marsh type and zone; see *SI Appendix*, Table S3 and Fig. S5 for site information and physical characteristics), and recorded mussel mortality due to predation. Mussel predation rates were highest in grazed border zones (66 ± 4% consumed; all mean ± SE), intermediate in marsh platforms adjacent to grazed creeks (32 ± 4% consumed) and ungrazed creek border zones (35 ± 4% consumed), and lowest on platforms adjacent to ungrazed creeks (17 ± 4% consumed; Creek Status*Marsh Area: $F_{1,83} = 4.6$; $P = 0.035$; Tukey's HSD, $P < 0.01$; Fig. 5*A*).

To experimentally assess how the presence of grazed creeks might influence predation on the most abundant ecosystem engineering marsh fauna, we selected three pairs of grazed and ungrazed marshes on Sapelo Island, GA, and tethered individual mussels and snails (*Littoraria irrorata*) in the following three treatments: 1) mesh cages sealed to the marsh sediment–water interface that excluded nekton and benthic predators (hereafter, full cage); 2) procedural cage controls (i.e., full cages elevated 15 cm above the marsh surface to allow predator access, but induce physical effects of cages); and 3) uncaged controls (hereafter, control). We selected mussels and snails due to their high abundance and ecological importance in southeastern salt marshes (62), as well as their complementary life-history traits (e.g., sessile vs. mobile) that moderate their exposure to predators. Observations of crushed mussels and plucked or crushed snail shells indicated that predation, rather than desiccation, was the primary cause of mortality in this experiment that spanned 4 wk of moderate temperatures and rainfall (*SI Appendix*, Fig. S5).

Classification tree analyses (63) explained 78% and 77% of the variation in mussel and snail survivorship, respectively, and revealed that the mortality of both species was low (2% of mussels and 3% of snails died) in full cages that excluded all predators, but varied with landscape context in treatments exposed to predation (Fig. 5*B*). In ungrazed creeksheds, consumption of tethered individuals by predators was low (31% of mussels and 44% of snails) across both border and platform locations. In contrast, predation was very high for both invertebrate functional groups when they were deployed near grazed creeks. Predation was highest on grazed borders (83% of mussels and 75% of snails) and intermediate on grazed platforms (52% of mussels and 46% of snails). These results provide experimental confirmation that, associated with the removal of the creekhead tall-form cordgrass barrier and longer tidal-submergence times, predation pressure is higher, and, hence, marsh fauna survivorship is lower on marsh platform locations associated with grazed creeks.

Evaluation of *Sesarma*'s Keystone Status. Finally, to evaluate whether the ecological and eco-geomorphic impacts of *Sesarma* qualify this once-inconspicuous grazer as a "keystone" species, we calculated *Sesarma*'s community importance in regulating several ecosystem functions and processes (5). Species whose effects on ecological traits are directly proportional to their abundance or biomass have community importance values equal to +1 or −1, with the sign of community importance indicating whether the focal species enhances or depresses the ecosystem trait of interest, respectively (5). Keystone species are those with absolute community importance values far greater than 1, reflecting disproportionately large ecological effects. Although

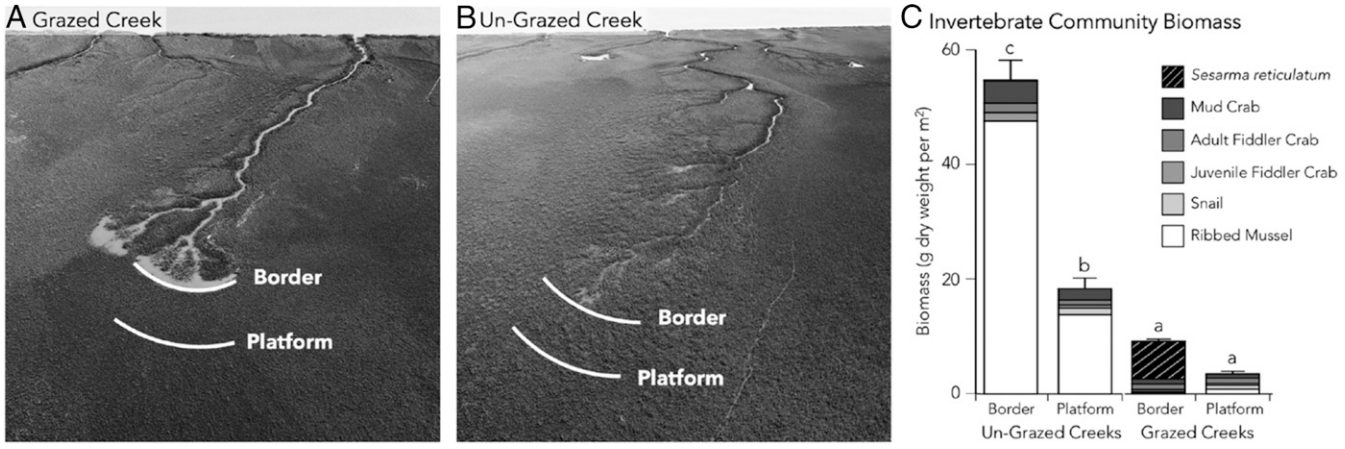

Fig. 4. *Sesarma* effects on invertebrate communities. Surveys of the border and platform zones in *Sesarma*-grazed (*A*) and ungrazed marshes (*B*) reveal differences in invertebrate community biomass and composition (*C*). In *C*, grayscale colors denote macrobenthic invertebrate functional groups comprising the community, and column heights and error bars represent the mean invertebrate biomass ± SE, respectively, of 56 replicate survey quadrats per marsh type and zone; values were averaged across regional sites because no significant effect of site was found. Image credit: C. Ortals.

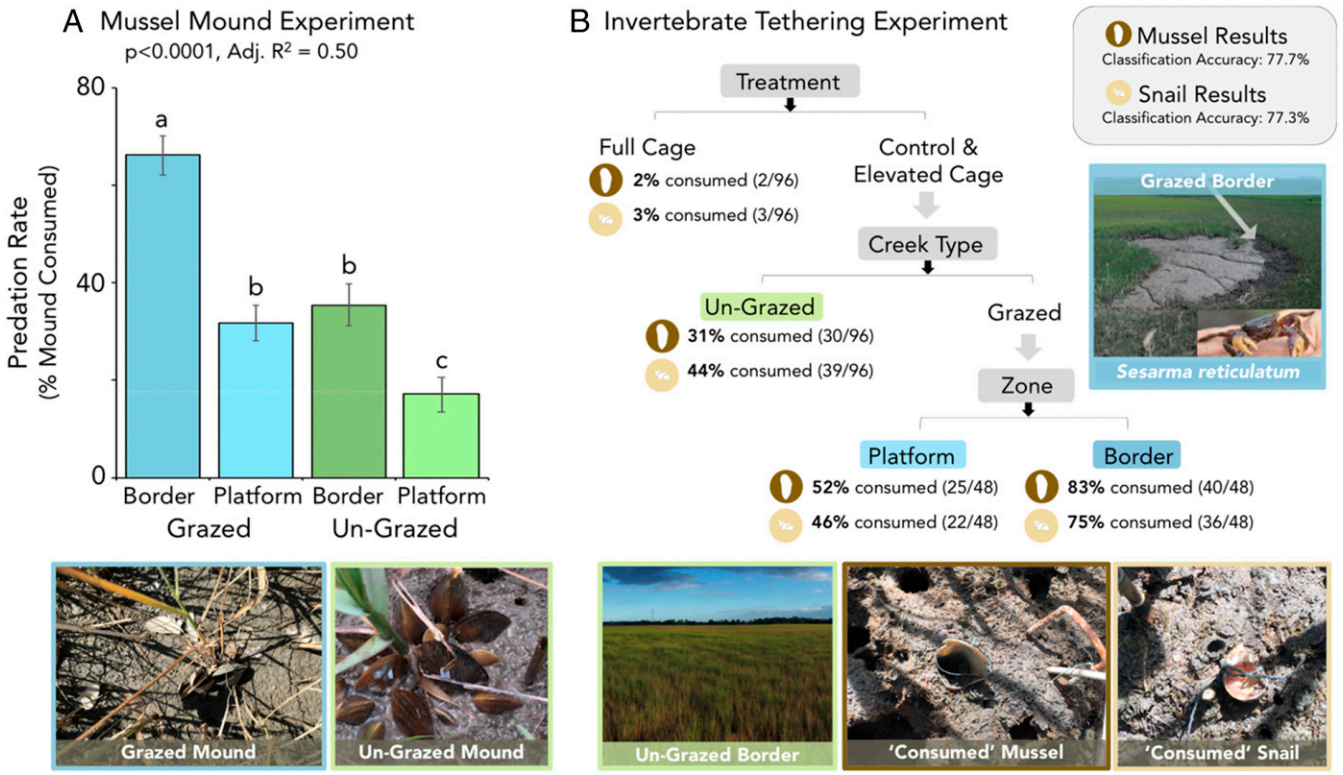

Fig. 5. Experimental results. (*A*) The predation rate on mussel aggregations deployed on grazed (blue) and ungrazed (green) creek borders and marsh platforms, reported as the percent of each mussel aggregation consumed after 4 wk (data are shown as the mean ± SE of eight aggregations per creek type and zone; data are pooled across three sites). (*B*) Classification tree analysis of predation rates on mussels (dark brown icons) and snails (light brown icons) revealed a hierarchy of factors controlling benthic macroinvertebrate survival. For both mussels and snails, predator exclusion (i.e., full cage vs. control and elevated cage) explained the greatest degree of variance in the data, followed by creek type (i.e., ungrazed vs. grazed) and then zone (i.e., platform vs. border).

Sesarma likely functions as a dominant species (5) at the local scale of a grazing front (m^2) due to its high abundance and proportionately strong direct ecological impacts in these confined locations (*SI Appendix*, Fig. S6), we focus our analyses of *Sesarma*'s community importance on the creekshed scale encompassing both border and platform zones, given the greater relevance of this spatial scale to *Sesarma*'s overall effects (both direct and indirect) on marsh structure and function. *Sesarma*'s community importance values, averaged across border and platform zones to provide an integrated summary of this species' creekshed-scale impacts, were all considerably greater than ±1 and differed in direction and magnitude across traits (Fig. 6*A*). While *Sesarma* reduce cordgrass biomass through their grazing and burrowing activities (community importance = −2.02), they have far stronger negative effects on mussel survivorship (community importance = −8.81) and invertebrate community biomass (community importance = −31.15), traits that this species controls indirectly via its localized removal of the predation-alleviating canopies of cordgrass and modification of tidal submergence. We also found that *Sesarma*'s enhancement of creek-elongation rates, an eco-geomorphic process that this crab directly enhances through its bioturbation and grazing activities (31–33), was disproportionately large relative to its biomass (community importance = +11.1; Fig. 6*A*). Combined, these results indicate that where sea-level rise has provided the context for *Sesarma* grazing fronts to establish and propagate, historic salt-marsh community dynamics (Fig. 6*B*) are fundamentally reorganized. Through both direct and indirect ecological and geomorphic effects (Fig. 6*C*), this emergent keystone grazer is reshaping landscape predator–prey dynamics and the mechanisms through which these intertidal landscapes are geomorphically responding to global climate change.

Conclusions

These findings provide evidence that the geospatial evolution, structure, and function of salt marshes spanning the southeastern US coastal plain are changing rapidly due to sea-level rise and the emergence of a keystone species, *S. reticulatum*. Although other dimensions of global change also occurring in the region, such as eutrophication, drought, and changes in food web structure (30), may be contributing to *Sesarma*'s rise in community importance, sea-level rise amplifying the dual functionality of *Sesarma* as a grazer and sediment engineer appears to be the critical factor activating its keystone status. Indeed, rising sea levels are pervasively enhancing tidal-submergence levels and water velocities in salt marshes across this region, a physical regime that both attracts this burrowing herbivore to well-flushed and oxygenated sediments on creekheads (31, 33) and intensifies its bioturbation impacts by making marsh-platform substrates softer and, hence, easier for *Sesarma* to excavate (29). Once concentrated on creekheads, our mortality assay and tethering experiments indicate that *Sesarma* overgrazing of the plant canopy and consequential enhancement of invertebrate exposure to top-down control is altering the functionality of these coastal wetlands as nursery and foraging grounds in areas that extend far beyond the relatively small footprint of the grazing front. Collectively, these results challenge the conventional perception that foundational cordgrass is the sole species of importance in controlling predator access and the resulting ecological community structure across elevations and tidal

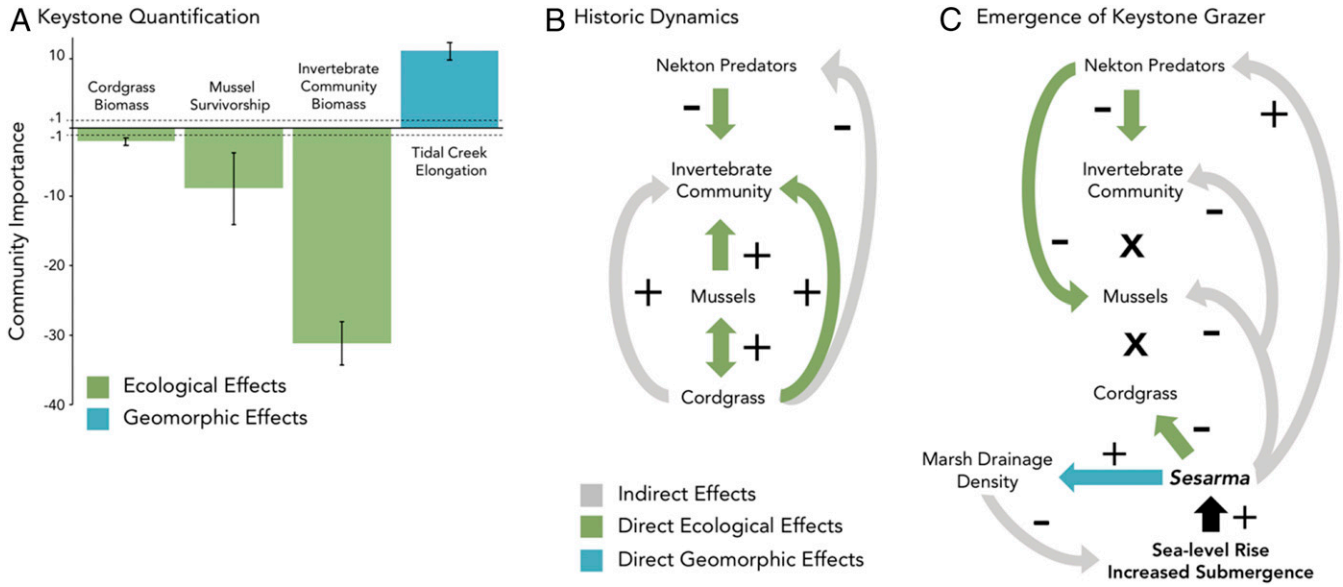

Fig. 6. *Sesarma*'s community importance and effects on salt-marsh interaction networks. (*A*) *Sesarma*'s community importance in controlling cordgrass biomass, mussel survivorship, macrobenthic invertebrate community biomass, and creek elongation, averaged across border and platform zones at the three Sapelo Island sites. All data are shown as mean ± SE of a minimum of 24 replicate measurements per grazed and ungrazed creekshed assessed for each factor. Positive community importance reflects an increase in the metric, while negative values reflect a decrease in the metric when *Sesarma* are present in higher density (grazed creeks) as compared to lower densities (ungrazed creeks). Species with community importance values far greater than ±1 (denoted by dashed lines) are considered "keystone" species. (*B* and *C*) Conceptual diagram summarizing the likely differences in species interaction networks in southeastern US Atlantic salt marshes in this "historic" period of 1940 to 1999 (*B*) vs. the contemporary period of 1999 to 2019 when *Sesarma*-grazed creeks have become prevalent features (*C*) due to *Sesarma*'s direct and indirect effects (colored and gray arrows, respectively) on other community members.

submergence gradients (e.g., refs. 59 and 64), as well as tidal-creek geomorphic evolution in salt marshes (e.g., refs. 65 and 66). Instead, our findings indicate that sea-level rise is amplifying *Sesarma*'s sediment-excavation and grazing impacts, enabling this animal with historically modest ecological effects relative to its population size (44–49) to function at levels of importance on par with cordgrass in defining the ecosystem's structure, function, and response to rising sea levels (Fig. 6).

Importantly, whether *Sesarma*'s current keystone status is ephemeral and which factors beyond those identified herein may be interacting with sea-level rise to control spatial and temporal variation in this crab's community importance remain outstanding questions. Since the term "keystone species" was coined by Robert Paine (1969) (6), ecologists have been scrutinizing the context dependency of keystone species. Indeed, it is well-appreciated that naturally occurring climate cycles, such as shifts in water temperature invoked by El Niño–La Niña cycles (7); stress gradients, such as variation in wave exposure along rocky shores (67); and disturbance events, such as wildfires (68), dictate whether a species will or will not function as a strong-interacting keystone (for a summary of examples, see ref. 5). Thus, our research complements and builds upon this foundational research on "contingent" keystone species by highlighting that such context dependency in a species' community importance can arise not only due to natural climate cycles, stress gradients, and disturbance, as has been historically emphasized, but also due to the novel environmental conditions being generated via global change. Given how pervasively sea-level rise, nutrient pollution, drought, and other dimensions of global change are altering environmental conditions (69), it is likely that the environmental context defined by global change may now be the most important factor controlling which organisms are functioning as keystones and, more generally, what physical and biotic factors will define community patterns and ecosystem functions going forward.

Beyond the southeast US coastal plain, sea-level rise is altering the magnitude and spatial distribution of material and propagule fluxes through intertidal and shallow subtidal ecosystems, thereby redefining the gradients in physical and biotic stresses that have long characterized these systems (70–72). In changing the environmental templates upon which species interact, this globally relevant manifestation of climate change is likely redefining the spatial distribution and community importance of many other organisms with previously weak ecological effects, as well as the historically dominant biota, such as foundational marsh grasses, algae, oysters, and corals, in coastal and nearshore landscapes worldwide. Inspired by our results, we hypothesize that species that function as particularly powerful ecosystem engineers (73–75), either by interacting strongly with foundation species (as mutualists, grazers, or bioeroders) or by interacting strongly with sediments, such as bioturbators or biodepositers, are prime candidates to emerge as keystone species in the context of sea-level rise or other dimensions of global change. This is because the direct effects of these organisms will have high potential to cascade through ecosystems via removal or enhancement of the ecosystem-defining foundation species, pronounced effects on sediment accumulation or erosion processes, and/or their alteration of the ecosystem's underlying geomorphic structure and the feedbacks that maintain it. Additional work is now needed to test this hypothesis and, more broadly, to identify emerging keystone species in other systems where global change is similarly altering the stress regimes, spatial organization, and/or interaction networks that historically shaped the system. Identifying general patterns in keystone emergence—and the mechanisms through which they alter the structure and function of ecosystems—will be crucial for informing predictions of ecosystem stability, functionality, and persistence as global stressors overlap and interact in the Anthropocene.

Methods

Sea-Level Rise, Marsh Accretion, and Tidal Submergence. To explore how sea-level rise may be altering the inundation regime of salt marshes, we obtained data from NOAA tide stations at three locations: Charleston Cooper River Entrance (SC), Fort Pulaski (GA), and Fernandina Beach (FL). We calculated the mean annual rate of sea-level rise for two time periods, 1940 to 1998 (T1) and 1999 to 2019 (T2). We analyzed these time periods separately to allow us to compare how recent dynamics overlapping with the time period spanning the aerial-image analyses differed from those previously experienced by this system. For the same regions, we acquired all available measurements of salt-marsh-platform vertical-accretion rates through a literature search and contacting researchers with expertise in collecting such data. Measurements of vertical accretion were collected via radiometric dating of soil cores (^{210}Pb and ^{137}Cs; $n = 28$ locations), feldspar marker horizons ($n = 8$ locations), and SET measurements ($n = 19$ locations; *SI Appendix*, Table S1).

To assess how historic trends in sea level and vertical marsh accretion rates influence the duration that salt marshes are tidally submerged, we estimated the proportional change in submergence time at the average elevation of creekhead-platform borders (+0.40 m ASL). We focused on the creekhead-platform border ("0 m"), rather than the relatively lower-elevation inner creekhead or the higher-elevation marsh-platform zones (*SI Appendix*, Fig. S7), given that this is both the elevation and physical location where active *Sesarma* grazing and burrowing fronts are most prevalent (31, 33). To do so, we used a simplified approximation of submergence time on the marsh platform, which assumes that water depth is equal to measured hourly water level subtracted by the platform elevation. Using Matlab (Version 2019a), we downloaded all available data from the Fort Pulaski NOAA site at hourly intervals from 1940 to 2019. To account for accretion, we selected five scenarios representing the average minimum (0 mm·y^{-1}), average SET (1 mm·y^{-1}), mean (2.5 mm·y^{-1}), sea-level rise equivalent (2.9 mm·y^{-1}), and average maximum (4 mm·y^{-1}) accretion scenarios measured throughout the region (*SI Appendix*, Table S1). For each scenario, we generated an accretion vector, whereby the 1940 creekhead elevation started at +0.40 m ASL and increased annually by the prescribed accretion-rate value. For each year, we then calculated inundation times by subtracting water level (height) from creekhead elevation (+0.40 m ASL plus accretion per year). All resulting values of water levels ≤0 m were considered "dry." For each year with available water-level data, we calculated the average daily submergence time. Linear regression models were then fit to each of the five accretion scenarios in each time period, with year as the predictor variable and mean daily inundation time as the response variable.

Grazing Prevalence, Creek Elongation, and Marsh Drainage Density. We selected nine sites for the aerial-image analyses based on their relatively even spatial distribution across the southeastern US Atlantic coastline. At each site, we identified and delineated 1-km^2 areas in Google Earth that contained >95% cover of salt-marsh habitat dominated by cordgrass. To assess whether the prevalence of grazed creeks has been increasing recently across the region, we quantified the number of creekheads in each of the 1-km^2 areas at two time points and categorized each creekhead as grazed or ungrazed based on the presence of a denuded, semicircular, or fan-shaped mudflat along the headward margin, or creekhead, a feature that is generated exclusively by *Sesarma* grazing and burrowing fronts (e.g., Fig. 4*A* and *SI Appendix*, Fig. S7). Time points were selected based on the availability and quality of aerial imagery at each site (TP1: 1994 or 1999; TP2: 2016, 2017, or 2018). To verify that our designations of grazed and ungrazed creeks were accurate, we randomly selected a total of 15 grazed and 15 ungrazed creeks in the 2016 Google Earth images of both the Sapelo Island and Brunswick sites and visited these creeks in May 2017. We correctly designated all 60 creeks. This process was repeated at the remaining sites, except that only five grazed and five ungrazed creeks were visited to verify creek-type designations due to time constraints. All creek-type designations (i.e., grazed and ungrazed) based on the aerial images were accurate.

To next test the hypothesis that grazed creeks consistently elongate faster than ungrazed creeks, as suggested in prior studies of a few isolated creeks in a single South Carolina marsh (31, 32), we delineated the total length of all creeks located within the nine 1-km^2 areas. Similar to the method used by Hughes et al. (31), we utilized the path-measurement tool in Google Earth to quantify the length of each. Creek elongation rate (meters per year) was calculated as: [Final Length − Initial Length]/number of years between TP1 and TP2. This process was repeated for all tidal creeks within our nine regional sites (265 grazed and 660 ungrazed creeks). Finally, to test the hypothesis that grazed creek prevalence explains regional changes in landscape marsh drainage density, we summed all creek lengths in each of the nine sites at each time point and divided each value by 1 km^2, the area of each site delineated for our analyses and the approximate area of salt marsh drained by the creeks.

Geospatial Drivers of *Sesarma*-Grazed Creekhead Distribution. To assess whether the spatial distribution of *Sesarma*-grazed creekheads are nonrandom and associated with geospatial features known to control tidal fluxes through the marsh (76), we selected a subset of creeks from the aerial-image analysis. Using a random-number generator, we identified 20 creeks of each of the following three classes distributed across the nine sites: 1) ungrazed, 2) grazed, and 3) ungrazed at TP1 but grazed at TP2 (hereafter, "incipient grazed"). For each creek, we scanned the marsh area landward of its creekhead and then measured the straight-line distance (*L*) from the creekhead to either the next creekhead, creekbank, or high marsh border, selecting whichever feature was closest to the creekhead. Next, at a 90-degree angle relative to the line-feature *L*, we measured the width, *W*, or distance on both sides of the creekhead to the nearest edge feature (i.e., creek, creekhead, or marsh border) (*SI Appendix*, Fig. S8*A*). We then estimated each creek's associated marsh-platform area using the equation for the area of an oval, using measured axes *L* and *W* in the calculation. Finally, we divided the marsh-platform area by creek length to quantify the drainage ratio. To assess whether a threshold drainage ratio exists above which grazing commences, we identified two groups of "marginal creeks"—i.e., the five ungrazed creeks with the highest drainage ratios and the five incipient-grazed creeks with the lowest drainage ratios. We then used a linear regression analysis between creek length and platform area for each set of marginal creeks and assessed the slope of these regression lines, i.e., the platform area divided by the creek length, or the threshold drainage ratio. While the *y* intercept of the linear relationships for marginal grazed and ungrazed creeks differed (3,057 and 2,096, respectively), the magnitude of this difference was small relative to the variation in creekshed area measured across all creeks in our dataset (50,390 ± 7,913; mean ± SE).

Finally, leveraging our own field observations, we identified five previously grazed creeks that appeared to be transitioning back from grazed to ungrazed status, as cordgrass was actively expanding into the previously denuded, fan-shaped mudflat. This revegetation process leaves only a narrow band of burrowed marsh at the creekhead (*SI Appendix*, Fig. S8*B*). For creek selection, we inspected aerial images and verified that each creek exhibited classic features of an active *Sesarma* front (i.e., a semicircular, fan-shaped mudflat and creek elongation rates exceeding 1.5 m per y) from the late 1990s to mid-2000s, but in the last 3 to 5 y, experienced closure of the mudflat due to cordgrass colonization and slower elongation (<0.5 m·y^{-1}). For these creeks, we measured the drainage ratios in both 1999 (when the *Sesarma* front was highly active) and in 2019 (when the front was transitioning back to an ungrazed state) using the aforementioned methods. We then compared these drainage ratios to the threshold identified for sustaining *Sesarma*-grazing fronts.

Creek Morphology, Tidal Submergence, and Marsh Softening. To investigate how inundation may differ across creeksheds that occupy the same vertical elevation, but differ in their drainage ratios, we applied the ROMS. ROMS is a three-dimensional, free-surface, terrain-following numerical model that solves the Reynolds-averaged Navier–Stokes equations using hydrostatic and Boussinesq assumptions (57, 58). This circulation model has been used to evaluate estuarine circulation, the flooding of intertidal wetlands, and the effects of morpho-hydrodynamics and sea-level rise (77–81). Models consisted of a main channel, a marsh platform, a tidal creek, and outer marsh levees (see *SI Appendix, Supplementary Methods* for model parameters). To evaluate the effects of changing the drainage ratio, three idealized model bathymetries were considered. The bathymetries shared the same channel, levees, and marsh-platform areas, but differed in the length of the tidal creek, such that their drainage ratios were 849; 266; and 132 m^2 per m of tidal creek. To assess differences in tidal submergence experienced by the marsh surface, we selected a point standardized for both surface elevation (+0.7 m ASL) and distance to the creekhead (20 m) and quantified the total number of hours that point was submerged over one 12.42-h tidal cycle.

Finally, to understand how sea-level rise between 1940 and 2019 has affected submergence time at the threshold drainage ratio, we applied ROMS to the threshold drainage ratio at conditions representative of 1940 and 1999 and compared these values to those assessed in 2019. To do so, we subtracted Fort Pulaski (GA) average accretion rate (2.5 mm·y^{-1}) from the average rate of sea-level rise from 1940 to 1999 (2.9 mm·y^{-1}) and from 1999 to 2019 (6.4 mm·y^{-1}). We then multiplied these relative rates of sea-level rise (0.4 and 3.9 mm·y^{-1}) by the number of years in each time period considered (59 and 20 y, respectively) and then added these values to the base

bathymetry of the model simulations (2019 marsh elevation: +0.7 m ASL). ROMS were then conducted at the threshold drainage ratio of 266 m^2 per m of tidal creek by using elevated marsh platforms (+0.80 m in 1940 and 0.778 m in 1999) to simulate the increases in tidal submergence that occurred over time as a result of sea-level rise. To compare differences in submergence across the three time points, we calculated the percent change at the aforementioned point (i.e., standardized for both surface elevation [0.7 m] and distance to the creekhead [20 m]) on the model simulation in 1999 and 2019, as compared to the baseline inundation regime in 1940. Model results were then ground-truthed to assess accuracy of predictions (see *SI Appendix, Supplementary Methods* for ground truthing of geomorphology-based predictions).

***Sesarma* Effects on Community Structure and Species Interactions.** To assess invertebrate community structure associated with areas landward of grazed and ungrazed creeks, we conducted surveys at nine regional sites. At each of these sites, one pair of grazed and ungrazed creeks spaced <0.6 km apart and standardized for length was selected for the invertebrate community surveys based on accessibility. On Sapelo Island, we selected three creek pairs, which were located at Airport, Beach Road, and Little Sapelo marshes (*SI Appendix*, Table S3), sites that were also the locations for the mussel-mortality assay and tethering experiments. The Sapelo Island locations are similar to salt marshes across the study region with regards to the spatial distribution of cordgrass and invertebrates along their creek banks and interior marsh platforms (14).

At each creek, we randomly placed eight replicate quadrats (0.33 m × 0.33 m) along a 30-m transect that ran parallel the creek border and 20 m from this border in the marsh platform (Fig. 4 *A* and *B*). In each quadrat, we counted cordgrass stems and the number of snails (*L. irrorata*); mussels (*G. demissa*); juvenile and adult fiddler crab burrows (*Uca pugnax*, burrows <5 mm and >5 mm in diameter, respectively); mud crab burrows (*Panopeus herbstii* and *Eurytium limosum*); and *Sesarma* burrows. These represent the macrobenthic invertebrate functional groups observed across all surveyed sites. Juvenile and adult life stages were differentiated, given their significantly different size and functional differences (60). The two mud crab species were pooled because of their similar diet and burrowing behavior in these marshes. Crab burrows were identified based on distinct, visual characteristics (60). To estimate invertebrate community biomass, 10 individuals of each functional group were collected from Sapelo Island marsh sites, dried at 60 °C, and weighed. The entire body of crabs (carapace plus internal body tissue) was weighed, while the proportionately heavier shells of mussels and snails were removed, and just body tissues were weighed to provide more equitable assessments of biomass among functional groups. Macrobenthic invertebrate community biomass was calculated by multiplying density values by the average biomass per individual of each functional group and summing all functional group values.

To test whether mussel survival differed in marshes adjacent to grazed and ungrazed creeks, we transplanted mussels to mimic their natural distribution in dense aggregations (61). At each of the grazed and ungrazed creeks at the Sapelo Island sites, we transplanted mussels into aggregations of 15 individuals (three from each of five size classes: 30 to 39, 40 to 49, 50 to 59, 60 to 69, and 70 to 79 mm) in the border and platform zones. Mussels were scored as alive or predated (broken shell) every 3 to 4 d until 50% of individuals had died, which occurred after 28 d. This mortality assay ran from June 30 to July 29, 2016.

To further test the hypothesis that increased inundation regimes and the coincident removal of the cordgrass border enhances predator access to invertebrate marsh prey, we conducted a predator-exclusion tethering experiment across marsh zones. On June 15, 2016, we attached 15-cm-long braided fishing line tethers to individual mussels (shell height: 30 to 80 mm) and snails (shell height: 7 to 10 mm) with super glue and secured the other end of the tether to the marsh surface using a 10-cm garden staple in border and platform zones at three pairs of grazed and ungrazed creeks on Sapelo Island. Snails and mussels were deployed in one of three treatments: 1) full cages, 2) procedural cage controls, and 3) controls ($n = 8$ per treatment per zone per creek type). Treatments were spaced >0.75 m apart and randomly distributed in border and platform zones at each site. Cages were 10-cm-diameter galvanized wire mesh (1-cm^2 mesh size) cylinders that were either secured 3 cm into the substrate with wire staples (full cages) or elevated 15 cm above the substrate with bamboo stakes to enable predator access and capped with a lid of the same material. Temperature and evaporative water loss, metrics of potentially physiologically stressful environmental conditions, differed by <4% in full and elevated cages compared to open controls (*SI Appendix*, Fig. S9). Cages were 15 cm tall for sessile mussels and 30 cm tall for snails to enable these mobile individuals to freely climb cordgrass shoots. Each week for 4 wk, tethered organisms were scored as alive or dead. We considered snail and mussel individuals predated if their shells were crushed. At the conclusion of the experiment, we established eight 0.5 × 0.5-m permanent quadrats centered on each tethered mussel control ($n = 8$ replicates per zone per creek type per site). At the end of the growing season, we then harvested aboveground cordgrass from each of the quadrats, then washed, oven-dried, and weighed each sample in the laboratory to quantify crab-grazing effects on foundational plant primary production.

Evaluation of *Sesarma*'s Keystone Status. To determine if *Sesarma* have disproportionately large effects relative to their biomass, we calculated the community importance metric (*CI*) for four ecosystem functions using the equation:

$$\mathrm{CI} = \frac{\mathrm{Trait}_P - \mathrm{Trait}_A}{\mathrm{Prop}_P - \mathrm{Prop}_A} \times \frac{1}{\mathrm{Trait}_P}, \quad [1]$$

where *Trait* refers to a quantitative ecosystem function or community metric when the keystone is present (*P*) or absent (*A*), and *Prop* refers to the proportional biomass of the focal species (in our case *Sesarma*) relative to the biomass of all other species in areas where the keystone is either present (*P*) or absent (*A*) (5). We selected three ecological trait responses quantified in this study: 1) aboveground cordgrass biomass (g of dry weight per 0.25 m^2) from our end-of-growing-season plant samples, 2) mussel survivorship (percent of tethered open controls) from our tethering experiment, and 3) associated macrobenthic invertebrate community biomass (g per 0.11 m^2) from our invertebrate composition survey; and one biogeomorphic trait response: tidal creek growth (meters per year) from our aerial-image analysis. To evaluate *Sesarma*'s community importance at the creekshed scale, we averaged each ecological trait measured in both the border and platform zone. *Sesarma* community importance was calculated for all three biological ecosystem functions at each of the three experimental creek sites on Sapelo Island, for a total of three replicate grazed and three ungrazed creeks. *Sesarma* community importance for creek elongation was calculated for each of nine regional sites.

Statistical Analyses. Following our aerial-image analysis, to evaluate whether *Sesarma*-grazed creekheads increased in prevalence between TP1 and TP2 at each of nine regional sites, we used a one-way ANOVA with main effect time point (TP1 and TP2). Creek elongation was analyzed with a two-way fully factorial ANOVA, with main effects site and creek status (grazed or ungrazed). We then assessed the effect of grazing prevalence (percent of creeks grazed TP2) on drainage-density enhancement (percent) with linear regression analysis. Drainage ratios were square-root transformed to meet the assumptions of parametric statistics and analyzed with a one-way ANOVA with creek type as the main factor.

Community biomass, aboveground cordgrass biomass, mussel-assay predation rates, and align rank-transformed surface-elevation data were all separately analyzed by using a three-way ANOVA, with site, creek status, and zone treated as main factors. All post hoc analyses were completed by using Tukey's HSD test with Bonferroni-corrected *P* values in STATA SE (Version 15.1). Classification tree analysis (rpart, R, Version 3.1.0) was used to quantify the relative importance of treatment, site, creek type, and zone for explaining patterns in mussel and snail tethering consumption. This analysis was selected for our binary response variable in order to assess and visually demonstrate the hierarchy (and relative importance) of experimental, biological, physical, and geomorphic factors controlling invertebrate fate under each of the environmental contexts. Over-fitted trees were pruned using k-fold cross-validation (rpart, R, Version 3.1.0; ref. 63).

Materials and Correspondence. All requests for materials or additional details should be directed to S.M.C.

Data Availability. All datasets are freely available at https://doi.org/10.6084/m9.figshare.12581579.v1.

ACKNOWLEDGMENTS. This work was supported by NSF CAREER Grant 1652628 and NSF EAGER Grant 1546638 (to C.A.); NSF Graduate Research Fellowship Program Grant 1315138 (to S.M.C.) and the Voss Environmental Fellowship (to T.M.P.). Logistical support was provided by Georgia Coastal Ecosystems Long Term Ecological Research Station, the University of Georgia Marine Institute, and the Sapelo Island National Estuarine Research Reserve.

1. G. R. Walther *et al*., Ecological responses to recent climate change. *Nature* **416**, 389–395 (2002).
2. P. Kareiva, S. Watts, R. McDonald, T. Boucher, Domesticated nature: Shaping landscapes and ecosystems for human welfare. *Science* **316**, 1866–1869 (2007).
3. J. A. Estes *et al*., Trophic downgrading of planet Earth. *Science* **333**, 301–306 (2011).
4. B. Worm, R. T. Paine, Humans as a hyper keystone species. *Trends Ecol. Evol.* **31**, 600–607 (2016).
5. M. E. Power *et al*., Challenges in the quest for keystones. *Bioscience* **46**, 609–620 (1996).
6. R. T. Paine, A note on trophic complexity and community stability. *Am. Nat.* **103**, 91–93 (1969).
7. E. Sanford, Regulation of keystone predation by small changes in ocean temperature. *Science* **283**, 2095–2097 (1999).
8. S. A. Woodin *et al*., Same pattern, different mechanism: Locking onto the role of key species in seafloor ecosystem process. *Sci. Rep.* **6**, 26678 (2016).
9. D. Wohlgemuth, M. Solan, J. A. Godbold, Species contributions to ecosystem process and function can be population dependent and modified by biotic and abiotic setting. *Proc. Biol. Sci.* **284**, 20162805 (2017).
10. J. A. Estes, J. F. Palmisano, Sea otters: Their role in structuring nearshore communities. *Science* **185**, 1058–1060 (1974).
11. W. J. Ripple, E. J. Larsen, R. A. Renkin, D. W. Smith, Trophic cascades among wolves, elk and aspen on Yellowstone National Park's northern range. *Biol. Conserv.* **102**, 227–234 (2001).
12. M. E. Power, W. J. Matthews, A. J. Stewart, Grazing minnows, piscivorous bass, and stream algae-dynamics of a strong interaction. *Ecology* **66**, 1448–1456 (1985).
13. A. Rosenblatt *et al*., The roles of large top predators in coastal ecosystems: New insights from long term ecological research. *Oceanography* **25**, 140–149 (2012).
14. C. Angelini *et al*., A keystone mutualism underpins resilience of a coastal ecosystem to drought. *Nat. Commun.* **7**, 12473 (2016).
15. J. de Fouw *et al*., A facultative mutualistic feedback enhances the stability of tropical intertidal seagrass beds. *Sci. Rep.* **8**, 12988 (2018).
16. D. T. Iles, R. F. Rockwell, D. N. Koons, Reproductive success of a keystone herbivore is more variable and responsive to climate in habitats with lower resource diversity. *J. Anim. Ecol.* **87**, 1182–1191 (2018).
17. H. K. Lotze *et al*., Depletion, degradation, and recovery potential of estuaries and coastal seas. *Science* **312**, 1806–1809 (2006).
18. C. D. G. Harley, Climate change, keystone predation, and biodiversity loss. *Science* **334**, 1124–1127 (2011).
19. E. McLeod *et al*., A blueprint for blue carbon: Toward an improved understanding of the role of vegetated coastal habitats in sequestering CO_2. *Front. Ecol. Environ.* **9**, 552–560 (2011).
20. E. B. Barbier *et al*., The value of estuarine and coastal ecosystem services. *Ecol. Monogr.* **81**, 169–193 (2011).
21. L.R. Pomeroy, R.G. Wiegert, *The Ecology of a Salt Marsh*, (Springer-Verlag, Berlin, Germany, 1981).
22. K. B. Gedan, B. R. Silliman, M. D. Bertness, Centuries of human-driven change in salt marsh ecosystems. *Annu. Rev. Mar. Sci.* **1**, 117–141 (2009).
23. B. R. Silliman, M. D. Bertness, A trophic cascade regulates salt marsh primary production. *Proc. Natl. Acad. Sci. U.S.A.* **99**, 10500–10505 (2002).
24. L. A. Deegan *et al*., Coastal eutrophication as a driver of salt marsh loss. *Nature* **490**, 388–392 (2012).
25. B. R. Silliman *et al*., Degradation and resilience in Louisiana salt marshes after the BP-Deepwater Horizon oil spill. *Proc. Natl. Acad. Sci. U.S.A.* **109**, 11234–11239 (2012).
26. O. Hoegh-Guldberg *et al*., Coral reefs under rapid climate change and ocean acidification. *Science* **318**, 1737–1742 (2007).
27. R. Feagin, D. Sherman, W. Grant, Coastal erosion, global sea-level rise, and the loss of sand dune plant habitats. *Front. Ecol. Environ.* **3**, 359–364 (2005).
28. T. C. Coverdale, A. H. Altieri, M. D. Bertness, Belowground herbivory increases vulnerability of New England salt marshes to die-off. *Ecology* **93**, 2085–2094 (2012).
29. S. M. Crotty, C. Angelini, M. D. Bertness, Multiple stressors and the potential for synergistic loss of New England salt marshes. *PLoS One* **12**, e0183058 (2017).
30. C. Angelini, S. G. van Montfrans, M. J. S. Hensel, Q. He, B. R. Silliman, The importance of an underestimated grazer under climate change: How crab density, consumer competition, and physical stress affect salt marsh resilience. *Oecologia* **187**, 205–217 (2018).
31. Z. J. Hughes *et al*., Rapid headward erosion of marsh creeks in response to relative sea level rise. *Geophys. Res. Lett.* **36**, L03602 (2009).
32. C. A. Wilson, Z. J. Hughes, D. M. FitzGerald, The effects of crab bioturbation on Mid-Atlantic saltmarsh tidal creek extension: Geotechnical and geochemical changes. *Estuar. Coast. Shelf Sci.* **106**, 33–44 (2012).
33. H. D. Vu, K. Wie Ski, S. C. Pennings, Ecosystem engineers drive creek formation in salt marshes. *Ecology* **98**, 162–174 (2017).
34. C. Holdredge, M. D. Bertness, A. H. Altieri, Role of crab herbivory in die-off of New England salt marshes. *Conserv. Biol.* **23**, 672–679 (2009).
35. T. C. Coverdale, M. D. Bertness, A. H. Altieri, Regional ontogeny of New England salt marsh die-off. *Conserv. Biol.* **27**, 1041–1048 (2013).
36. A. H. Altieri, M. D. Bertness, T. C. Coverdale, N. C. Herrmann, C. Angelini, A trophic cascade triggers collapse of a salt-marsh ecosystem with intensive recreational fishing. *Ecology* **93**, 1402–1410 (2012).
37. T. M. Pettengill, S. M. Crotty, C. Angelini, M. D. Bertness, A natural history model of New England salt marsh die-off. *Oecologia* **186**, 621–632 (2018).
38. R. F. Lee, M. E. Frischer, The decline of the blue crab: Changing weather patterns and a suffocating parasite may have reduced the numbers of this species along the Eastern seaboard. *Am. Sci.* **92**, 548–553 (2004).
39. C. H. Ernst, J. E. Lovich, *Turtles of the United States and Canada*, (Johns Hopkins University Press, Baltimore, MD, ed. 2, 2009).
40. A. Bortolus, O. O. Iribarne, The effect of the southwestern Atlantic burrowing crab *Chasmagnathus granulata* on a Spartina salt-marsh. *Mar. Ecol. Prog. Ser.* **178**, 79–88 (1999).
41. G. M. Perillo, O. O. Iribarne, Processes of tidal channel development in salt and freshwater marshes. *Earth Surf. Process. Landf.* **28**, 1473–1482 (2003).
42. J. M. Teal, Distribution of fiddler crabs in Georgia salt marshes. *Ecology* **39**, 185–193 (1958).
43. J. M. Teal, Energy flow in the salt marsh ecosystem of Georgia. *Ecology* **43**, 614–624 (1962).
44. L. G. Abele, Taxonomy, distribution and ecology of the Genus *Sesarma* (Crustacea, Decapoda, Grapsidae) in Eastern North America, with special reference to Florida. *Am. Midl. Nat.* **90**, 375–386 (1973).
45. W. Seiple, Distribution, habitat preferences and breeding periods in the crustaceans *Sesarma cinereum* and *S. Reticulatum* (Brachyura: Decapoda: Grapsidae). *Mar. Biol.* **52**, 77–86 (1979).
46. W. Seiple, The ecological significance of the locomotor activity rhythms of Sesarma cinereum (Bosc) and *Sesarma reticulatum* (Say) (Decapod, grapsidae). *Crustaceana* **40**, 5–15 (1981).
47. E. B. Haines, Relation between the stable carbon isotope composition of fiddler crabs, plants, and soils in a salt marsh. *Limnol. Oceanogr.* **21**, 880–883 (1976).
48. H. F. Sharp Jr., Food ecology of the rice rat, *Oryzomys palustris* (Harlan), in a Georgia salt marsh. *J. Mammal.* **48**, 557–563 (1967).
49. R. Kneib, Patterns of invertebrate distribution and abundance in the intertidal salt marsh: Causes and questions. *Estuaries* **7**, 392–412 (1984).
50. R. F. Dame *et al*., Estuaries of the South Atlantic coast of North America: Their geographical signatures. *Estuaries* **23**, 793–819 (2000).
51. D. R. Cahoon, R. E. Turner, Accretion and canal impacts in a rapidly subsiding wetland II. feldspar marker horizon technique. *Estuaries* **12**, 260–268 (1989).
52. J. Jarrett, "Tidal prism-inlet area relationships" (Tech Rep., U.S. Army Coastal Engineering Research Center, Fort Belvoir, VA, 1976).
53. S. A. Hughes, Equilibrium cross sectional area at tidal inlets. *J. Coast. Res.* **18**, 160–174 (2002).
54. A. D'Alpaos, S. Lanzoni, M. Marani, A. Rinaldo, On the tidal prism–channel area relations. *J. Geophys. Res.* **115**, F01003 (2010).
55. Z. Hughes, "Tidal channels on tidal flats and marshes" in *Principles of Tidal Sedimentology*, R. A. Davis Jr., R. W. Dalrymple, Eds. (Springer, Dordrecht, Netherlands, 2012), pp. 269–300.
56. S. M. Crotty, C. Angelini, Geomorphology and species interactions control facilitation cascades in a salt marsh ecosystem. *Curr. Biol.* **30**, 1562–1571.e4 (2020).
57. A. F. Shchepetkin, J. C. McWilliams, The regional oceanic modeling system (ROMS): A split-explicit, free-surface, topography-following-coordinate oceanic model. *Ocean Model.* **9**, 347–404 (2005).
58. D. B. Haidvogel *et al*., Ocean forecasting in terrain-following coordinates: Formulation and skill assessment of the Regional Ocean Modeling System. *J. Comput. Phys.* **227**, 3595–3624 (2008).
59. D. B. Lewis, L. A. Eby, Spatially heterogeneous refugia and predation risk in intertidal salt marshes. *Oikos* **96**, 119–129 (2002).
60. C. Angelini *et al*., Foundation species' overlap enhances biodiversity and multifunctionality from the patch to landscape scale in southeastern United States salt marshes. *Proc. Biol. Sci.* **282**, 1–9 (2015).
61. S. M. Crotty *et al*., Foundation species patch configuration mediates salt marsh biodiversity, stability and multifunctionality. *Ecol. Lett.* **21**, 1681–1692 (2018).
62. B. R. Silliman, J. van de Koppel, M. D. Bertness, L. E. Stanton, I. A. Mendelssohn, Drought, snails, and large-scale die-off of southern U.S. salt marshes. *Science* **310**, 1803–1806 (2005).
63. T. Therneau, B. Atkinson, B. Ripley, rpart. https://cran.r-project.org/web/packages/rpart/index.html. Accessed 5 October 2019.
64. R. F. Denno, D. L. Finke, G. A. Langellotto, "Direct and indirect effects of vegetation structure and habitat complexity on predator–prey and predator–predator interactions" in *Ecology of Predator–Prey Interactions*, P. Barbosa, I. Castellanos, Eds. (Oxford University Press, Oxford, UK, 2005), pp. 211–239.
65. A. D'Alpaos, S. Lanzoni, M. Marani, S. Fagherazzi, A. Rinaldo, Tidal network ontogeny: Channel initiation and early development. *J. Geophys. Res.* **110**, F02001 (2005).
66. S. Fagherazzi *et al*., Numerical models of salt marsh evolution: Ecological, geomorphic, and climatic factors. *Rev. Geophys.* **50**, RG1002 (2012).
67. B. A. Menge *et al*., The keystone species concept: Variation in interaction strength in a rocky intertidal habitat. *Ecol. Monogr.* **64**, 249–286 (1994).
68. H. T. Dublin, A. R. E. Sinclair, J. McGlade, Elephants and fire as causes of multiple stable states in the Serengeti-Mara Woodlands. *J. Anim. Ecol.* **59**, 1147–1164 (1990).
69. ; Intergovernmental Panel on Climate Change, *Climate Change 2014: Synthesis Report. Contribution of Working Groups I, II and III to the Fifth Assessment Report of the Intergovernmental Panel on Climate Change Core Writing Team*, R. K. Pachauri, L. A. Meyer, Eds. (IPCC, Geneva, Switzerland, 2014).
70. W. K. Michener, E. R. Blood, K. L. Bildstein, M. M. Brinson, L. R. Gardner, Climate change, hurricanes and tropical storms, and rising sea level in coastal wetlands. *Ecol. Appl.* **7**, 770–801 (1997).
71. T. Fujii, Climate change, sea-level rise and implications for coastal and estuarine shoreline management with particular reference to the ecology of intertidal benthic macrofauna in NW Europe. *Biology* **1**, 597–616 (2012).
72. D. L. Passeri *et al*., The dynamic effects of sea level rise on low-gradient coastal landscapes: A review. *Earths Futur.* **3**, 159–181 (2015).

73. T. S. Bianchi, C. G. Jones, M. Shachak, Positive feedback of consumer population density on resource supply. *Trends Ecol. Evol.* **4**, 234–238 (1989).
74. C. G. Jones, J. H. Lawton, M. Shachak, Organisms as ecosystem engineers. *Oikos* **69**, 373–386 (1994).
75. C. G. Jones, J. H. Lawton, M. Shachak, Positive and negative effects of organisms as physical ecosystem engineers. *Ecology* **78**, 1946–1957 (1997).
76. C. A. Wilson *et al.*, Salt marsh pool and tidal creek morphodynamics: Dynamic equilibrium of northern latitude salt marshes? *Geomorphology* **213**, 99–115 (2014).
77. D. A. Sutherland, P. Maccready, N. S. Banas, L. F. Smedstad, A model study of the Salish Sea estuarine circulation. *J. Phys. Oceanogr.* **41**, 1125–1143 (2011).
78. M. Olabarrieta, W. R. Geyer, G. Coco, C. T. Friedrichs, Z. Cao, Effects of density-driven flows on the long-term morphodynamic evolution of funnel-shaped estuaries. *J. Geophys. Res. Earth Surf.* **123**, 2901–2924 (2018).
79. J. C. Warner, Z. Defne, K. Haas, H. G. Arango, A wetting and drying scheme for ROMS. *Comput. Geosci.* **58**, 54–61 (2013).
80. E. E. Wheat, N. S. Banas, J. L. Ruesink, Multi-day water residence time as a mechanism for physical and biological gradients across intertidal flats. *Estuar. Coast. Shelf Sci.* **227**, 106303 (2019).
81. N. K. Ganju, D. H. Schoellhamer, Calibration of an estuarine sediment transport model to sediment fluxes as an intermediate step for simulation of geomorphic evolution. *Cont. Shelf Res.* **29**, 148–158 (2009).